"Experimental and Modelling Vortex Tube Performance"

Mohamed KALAL[1], Richard MATAS[2], Jiří LINHART[3]

[1] Corresponding Author. Department of Power System Engineering, Faculty of Mechanical Engineering, University of West Bohemia. Univerzitni 8, Plzen 306 14. Czech Republiy. Tel.: +420 377 63 8132, Fax: +420 377 63 8102, E-mail: kalal@kke.zuc.cz

[2] New Technologies Research Centre, University of West Bohemia. E-mail: mata@ntc.zcu.cz

[3] Department of Power System Engineering; Faculty of Mechanical Engineering, University of West Bohemia; E-mail: linhart@kke.zcu.cz

ABSTRACT

Vortex tube is a simple mechanical device operating as a refrigerating and heating machine with no moving parts**.** An experimental study of the vortex tube, using compressed air as the working medium, has been carried out to investigate the effect of thermo-physical parameters, which have been designated and studied. Atest facility specially built for this project. Experiment results of the temperature of the hot and cold air outlet of the vortex tube, with the cold air mass ratio (CAMR) and the pressure of the inlet air as parameters are presented. It is also shown that the inlet pressure and the CAMR are an important factors influence the performance of the vortex tube.

In this paper a computational fluid dynamics (CFD) package is used to investigate the performance and flow phenomena within a counter-flow vortex tube. A three-dimensional CFD model has been developed that successfully exhibits all of the general behavior expected from a vortex tube. Temperature and velocity profiles in vortex tube from the CFD model are presented. It was found that of turbulent model are suitable for vortex tube. The CFD model compared with data obtained from oure experiments. It is in reasonable agreement with experimental results.

Keywords: Cold temperature, CFD, Experiment, Hot temperature, Vortex tube

NOMENCLATURE

m_c [*kg/s*]   mass flow rate of the cold air
m_i [*kg/s*]   mass flow rate of the inlet air
T [^{o}C]   temperature
y [-]   cold air mass ratio
ΔT_c [^{o}C]   temperature differences between cold outlet air and inlet air
ΔT_h [^{o}C]   temperature differences between hot outlet air and inlet air

Subscripts
i   inlet
c   cold
h   hot

1. INTRODUCTION

The vortex tube creates a vortex from compressed air and separates it into two air streams, one hot and one cold. Compressed air enters a cylindrical generator, which is of proportionately larger diameter than the hot (long) tube where it causes the air to rotate. Then, the rotating air is forced to flow down the inner wall of the hot tube at speeds reaching a sonic value. At the end of the hot tube, a small portion of this air exits through a needle valve (control valve) as hot air exhaust. The remaining air is forced to flow back through the centre of the incoming air stream at a slower speed. The heat in the slower moving air is transferred to the faster moving incoming air, though here is a higher temperature. This cooled air flows through the centre of the generator and exits through the cold air exhaust port, as shown schematically in figure 1. The vortex tube can be used as a refrigeration device or as a heating device.
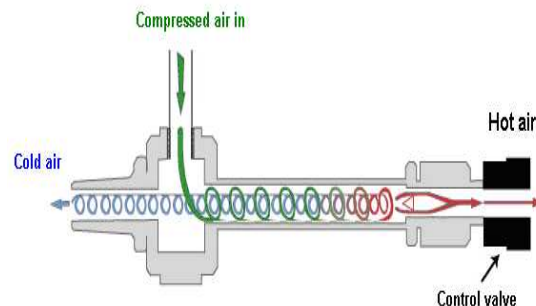

Figure 1. Schematic diagram of a vortex tube

[1] was the earliest one who investigated compressed air flowing tangentially into a tube and

found that air leaving near the wall had a higher temperature than that leaving near the axis. He tried to use this effect for refrigeration. [2] first published systematical experimental results by varying the inlet pressure and the geometrical parameters of the tube. A recent review of the existing literature is given by [3]. In spite of the present uses and the various studies, no adequate physical explanation is available for the actual transport mechanism. Indeed, in the existing literature, there have been several, often contradictory, qualitative theories. [4] assumed turbulent transfer of thermal energy in an incompressible flow. [5] invoked an acoustic streaming process. [6] identified the temperature splitting phenomenon of a Ranque–Hilsch vortex tube in which a stream of gas divides itself into a hot and a cold flow as a natural heat pump mechanism, which is enabled by a secondary circulation. [7] considered the vortex tube as a refrigeration device which could be analyzed as a classical thermodynamic cycle, replete with significant temperature splitting, refrigerant, and coolant loops, expansion and compression branches, and natural heat exchangers.

The effect of various parameters, such as nozzle area, cold orifice area, hot end area and L/D ratio of the tube length to the tube diameter, on the performance of the vortex tube was investigated in [8]. There were experimentally tested variations of the cold air temperature T_c with respect to the change of the hot end area for L/D = 45,50,55. They showed the cold air temperature T_c at all the tested ratios L/D decreased if the hot end was opened. Also the effects of length and diameter on the principal vortex tube are considered in [9]. They showed variation of efficiency versus different L/D of vortex tube. An experimental investigation of the energy separation process in the vortex tube was conducted in [10]. Showed measured the temperature profiles at different positions along a vortex tube axis and concluded that the length of the vortex tube would have an important influence on the transport mechanism inside. [11] is presented Experimental results of the energy separation in the vortex tube under different operating conditions, it showed the changes of the temperature of cold and hot streams as a function of the inlet pressure. In this study there was found that the temperature of the hot stream increased with the inlet pressure increasing, and that the temperature of the cold stream decreased with the inlet pressure. [12] resulted in several formulas for determining the performance and efficiency of vortex tubes under a variety of operating conditions, which induced the optimum ratios of vortex tube dimensions corresponding to the highest efficiency.

So far there is very plenty of available researches to validate the reliability of CFD analyses for investigating the flow and temperature withen the vortex tube. The numerical predictions qualitatively predicted the experimental results presented by [12]. [13,14] show the dependence of vortex tube performance on normalized pressure drop with a numerical model. [3.15] presents a numerical analysis in which the fluid dynamic equations are decoupled from the energy equation. The flow pattern was determined using the vorticity streamfunction formulation of the radial and axial Navier-Stokes equation and a standard k-ε turbulence model. CFD can also be used as a minimal adequate tool for design of engineering components. [16] Present a detailed analysis of various parameters of the vortex tube through CFD techniques to simulate the phenomenon of flow pattern, thermal separation, pressure gradient etc. And also its utility as a tool for optimal design of vortex tube towards the optimization of number of nozzles, nozzle profiles, cold end diameter, length to diameter ratio, cold and hot gas fractions and comparison of the experimental results with corresponding CFD analysis. [8] showed successfully utilized a CFD model of the vortex tube to understand the fundamental processes that drive the power separation phenomena. CFD and experimental studies are conducted towards the optimization of the Ranque– Hilsch vortex tubes are presented by [17]. They showed the swirl velocity, axial velocity and radial velocity components of the flow and the flow pattern have been obtained through CFD, The optimum cold end diameter and ratios of vortex tube length to diameter and optimum parameters for obtaining the maximum hot gas temperature and minimum cold gas temperature are obtained through CFD analysis and validated through experiments

2. EXPERIMENTAL SETUP

The arrangement of experimental apparatus and measuring devices which is used for the determination of the performance of the counter flow vortex tube is shown in figure 2. We have chosen model No. 106-8-H of the producer ITW Vortec. This model is one of the smallest, its air consumption is 0.00378 [kg/s], which corresponds to the maximum capacity of our compressor 0.005 [kg/s], with output pressure between 0.5 and 1.0 [M Pa]. The experimentation was started when the air was compressed from the air compressor (1), and supplied the high pressure air passes through the pressure tank (2) to suppress impacts and the valve (3), where its mass rate is regulated. Inlet pressure is read by the pressure gage (4) then goes through the dust filer (5) and cooler (6). The mass flow rate of the inlet air is measured using an orifice (7). Then the compressed air is introduced tangentially into the vortex tube (9), where it is expended and separated into hot and cold air streams. The cold air in the central region leaves the vortex tube near the entrance, while the hot air discharges the periphery at the far end of the vortex tube. The control valve

(needle valve)(10) may control the flow rate of the hot air. Just after the pipe, the mass flow rate of the hot air is measured using the orifice (12) Thermocouples numbered 8, 11 and 13 measure the temperatures of the inlet and outlet of the hot and the cold air in the vortex tube, respectively. All temperatures and pressures data were recorded with a data logger (14) on a PC (15). A program was written in LabVIEW 7.2 to control the data logging parameters and to display results obtained.
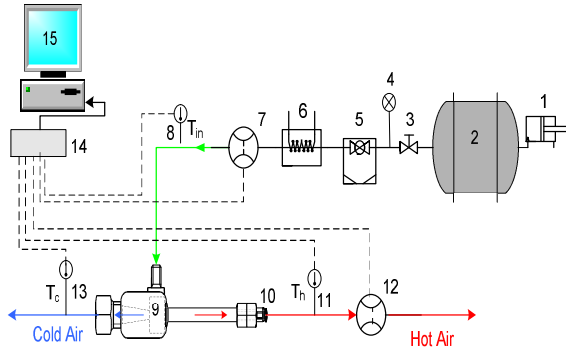

Figure 2: Schematic diagram of the experimental setup.

3. EXPERIMENTAL RESULT

During the experimental test, the inlet pressure and the inlet temperature of the compressed air as well as the cold air mass ratio y were varied systemically. The CAMR is defined as follows:

$y = \dot{m}_c / \dot{m}_i$, where $\dot{m}_c$ represents the mass flow rate of the cold stream released, while $\dot{m}_i$ represents the inlet or total mass flow rate of the pressurized inlet working fluid. Therefore, the CAMR changes in the range $0 \leq$ CAMR ≥ 1.

Tests have been conducted at inlet pressure of 2.7, 4, 6 and 8 bars, at constant inlet temperature 20°C . The experimental temperature of the hot and cold outlet air is shown in Figure 3 as a function of the cold air mass ratio and as a function of the inlet pressure of the compressed air.
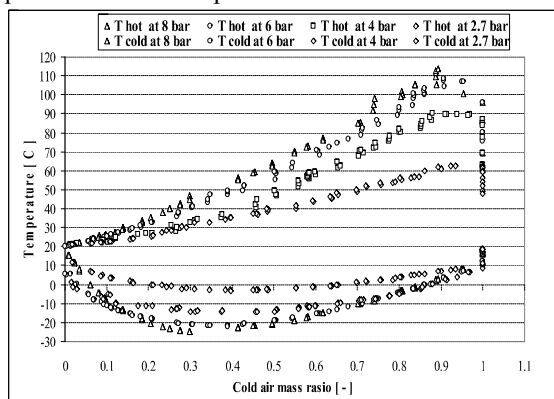

Figure 3. Hot and cold temperature as a function of cold mass ratio.

All tests were run at first by holding a constant inlet temperature. Obviously, it can be seen that the temperature of the exit air increases with increasing CAMR of Null up to nearly 0.85. With further increases of the cold air mass ratio higher than 0.85 the hot exit air temperature increases to a maximum value and then decreases to its minimum value. The range of the CAMR, at which the hot outlet air becomes a maximum, is from 0.85 to 0.90. At cold air mass ratio from 0.9 up to one sharp temperature drop is measured for the hot air exit temperature. Figure 3, gives also the temperature of the hot outlet air as a function of the inlet pressure as a parameter. At all CAMR the temperature of the hot air is proportional to the inlet pressure of air. In all the temperature of the vortex tube at the hot air exit is higher than that of the inlet air, $T_h > 20^{o}$C. In the range of CAMR of 1 up to 0.85, hence relative increases of the hot mass flow rate. The friction between the air molecular and the friction between the air and the pipe wall is very high so that the temperature of the hot otlet air increases and reaches its highest value. At CAMR lower than 0.85 more air flows into the hot outlet pipe. A decrease in the CAMR from 0.85 up to 0 causes a decrease in the wall friction effect; temperature drop as a consequence. With regard to the relationship between the temperature of the cold outlet air and the influencing parameters, as presented in Figure 3, it follow that the temperature of the cold outlet air decreases with increases CAMR up to 0.3 and reaches there a minimum value. While the temperature increases with further increases of the CAMR higher than 0.3.

From experimental results, it indicated that the temperature differences between the hot outlet air and the inlet air, $\Delta T_h = T_h - T_i$, and between the cold outlet air and the inlet air, $\Delta T_c = T_c - T_i$, as functions of the CAMR, with the pressure of the inlet air as a parameter are presented in figure 4. Without the outflow of the hot air, y = 1, the temperature of the vortex tube at the hot air outlet is higher than that of the inlet air. Similarly without the outflow of the cold air, y = 0, the temperature measured at the outlet of the cold air, is lower than the temperature of the inlet air. Also Figure 4 demonstrates that for CAMR in a range of 0.1 to 0.4, there is distinctively a potential of higher rate of temperature reduction in the cold outlet but lower rate of temperature reduction for the range beyond 0.4. For the CAMR in a range between 0.3 and 0.4, there is the highest rate of temperature reduction in the cold outlet for all inlet pressures supplied. When inlet pressures are at 2.7, 4, 6 and 8 bars, the highest rate of decreasing temperature in the cold outlet are 22°C, 33°C, 42°C and 46°C respectively. The higher the inlet pressure the more decreasing temperature for each CAMR used.
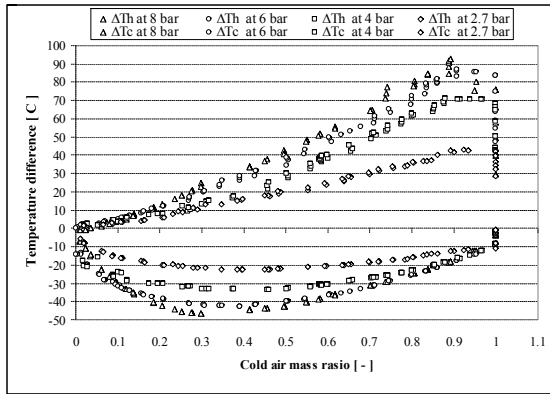
Figure 4. Hot and cold temperature differences as a function of cold mass ratio

The influence of the inlet pressure on the temperature of the hot and cold outlet air is clearly distinctive as shown in Figure 5. It can be seen that the temperature of the hot outlet increases with inlet pressure increasing, and that the cold outlet decreases with inlet pressure. The compressed air begins its vortex flow as soon as it is introduced into the vortex tube. Because of the centrifugal characteristics of the forced vortex flow, the tangential velocity of the air near the vortex tube wall would be larger than that in the central region. This would naturally cause the temperature near the tube wall to be higher than that in the central region. Also, the higher frictional force among fluid particles as well as among the fluid particles and the vortex tube wall near the wall region is responsible for part of this phenomenon. The higher the inlet pressure, the greater the centrifugal force. Then the difference between the tangential velocity in the near wall region and that in the central region would be larger, and hence the difference between the temperatures of the two outlets.
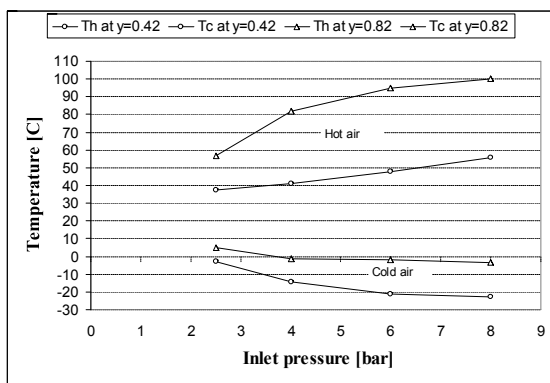

Figure 5. Hot and cold outlet temperature as a function of inlet pressure.

4. CFD COMPUTATIONS

The CFD system FLUENT in version 6.1 was used for numerical simulations numerical model was based on experiences with previous solved axisymetric models [18]. Geometry of the vortex tube simulated by a 3D CFD model is depicted in figure 6. The geometry come from the measured vortex tube and is simplified. The periodical segment (angle 60°) was used for the simpler solving; the hot outlet valve wasn't simulated completely, but the control valve was replaced by the pressure outlet with variable area.
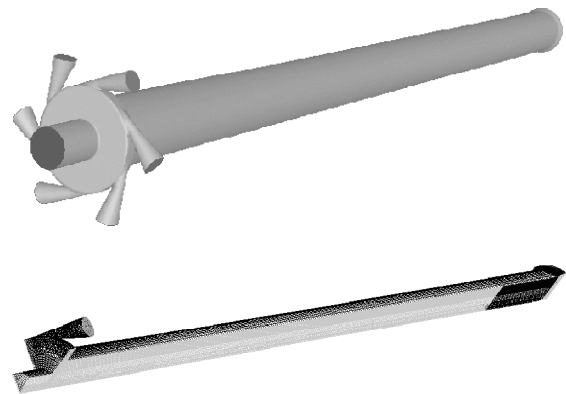

Figure 6. Geometry of the CFD model and computational mesh of the solved periodical segment

Computational mesh of the periodical segment has about 70 000 mixed cells. The parameters of the model were entered following: inlet mass flow 6.10^{-4} kg/s (one inlet nozzle), inlet total temperature 293 K, outlet pressure 95 600 Pa, walls was set adiabatic. The initialising of the computation must be set suitably to obtain converging solution. The computations converged relatively slowly, the number of iterations leading to a converged solution was more than 10 000.

The standard k-ε model was used, the relation between turbulent and laminar viscosity was reduced to 500 to obtain more realistic velocity profiles, see [18]. The inlet turbulent intensity in described model was set to 3 %. The turbulent Prandtl number in the turbulent model was incrrease. The performed simulations give the best results for $Pr_t = 9$, as in the work [16].

Computed results were satisfactory. The computed inlet total pressure for the given mass flow rate was 7.10^5 Pa. This value is less than which measured experiment value 8.10^5 Pa. Figure 7 shows radial – axial velocity field in the vortex tube for the CAMR 0.5183. It is possible to see the basic character of the flow field, which corresponds with the flow field described by other authors.
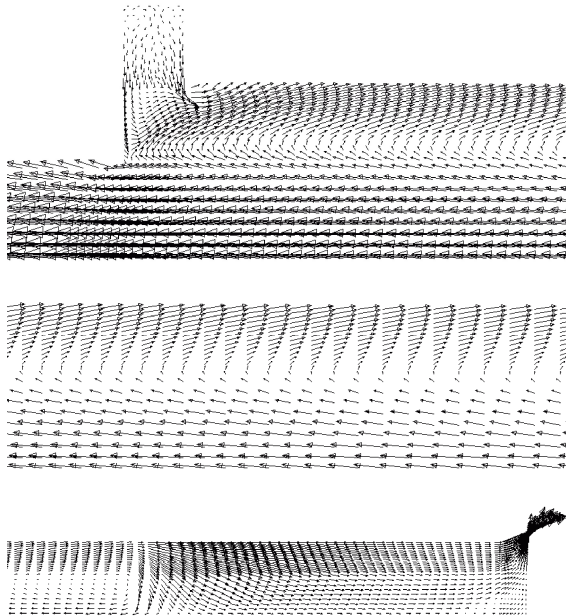
Figure 7. Velocity vectors without tangential component in various locations of the vortex tube for the cold fraction 0.5183

Figure 8. shows the radial – tangential velocity field in the plane of the inlet nozzles and shows the basic vortex. The performance of swirl generators can be characterised by two factors, namely the magnitude of swirl velocity and radial symmetry of flow.
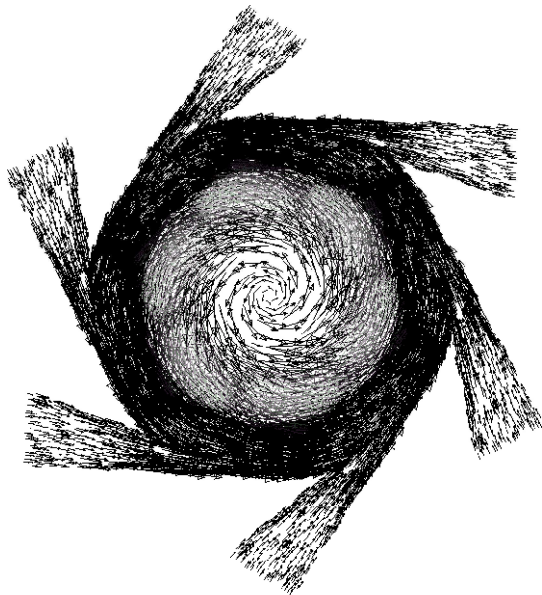

Figure 8. Velocity vectors without axial component in the plane of the inlet nozzles for the cold fraction 0.5183

Figure 9 shows the Tangential velocity profiles in the slice 0, 44 and 88 mm from the plane of the

inlet nozzles. It is seen degrease of the tangential velocity from the inlet and cold outlet to the hot outlet.
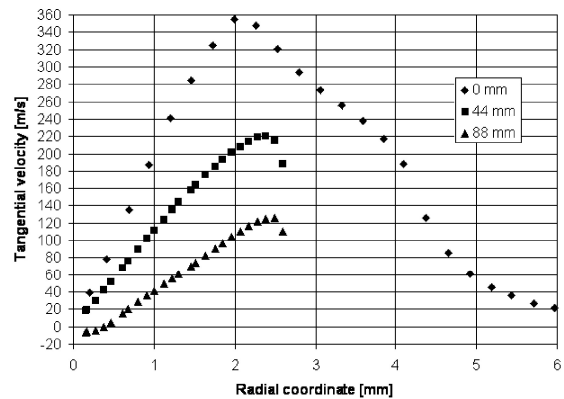

Figure 9. Tangential velocity profiles in the slice 0, 44 and 88 mm from the plane of the inlet nozzles for the cold fraction 0.5183

The distribution of the total temperature shows the figure 10. It is noticeable, that the increase of the total temperature from inlet to the hot outlet is relatively constant in the diameter 3.5 mm and the own increase of the temperature originates in the relatively thin layer round the wall of the vortex tube.
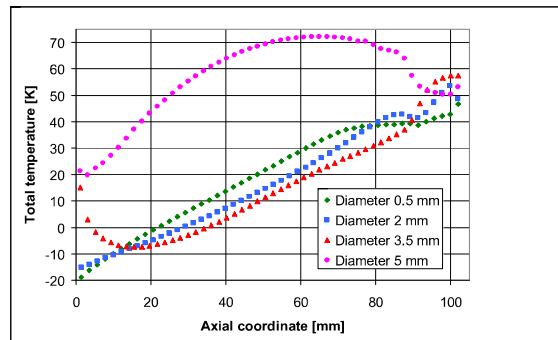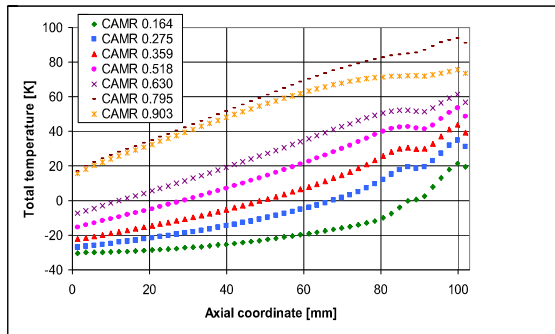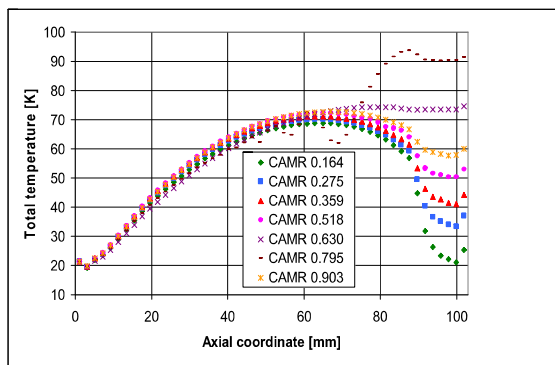

Figure 10. Total temperature profiles on the diameters 0.5, 2, 3.5 and 5 mm for the cold fraction 0.5183

In the figure 11 you can see the distribution of the total temperature in the tube for various CAMR. The behaviour of the tube is changed in the range 0.63 to 0.79 of the CAMR, where the temperature distribution has a different order.

(a)

(b)

Figure 11, Total temperature profiles for the various cold fractions: (a) for the diameters 2 mm (up) , (b) 5 mm (down)

5. COMPARISON BETWEEN EXPERIMENT AND CFD

The inlet temperature and inlet mass flow rate in the CFD model were specified as a constant 20 ^{o}C and 0.0036 kg/s respectively, which is consistent with the measured total temperature at the inlet to the vortex tube. The results of the experimental model were compared with two-dimensional, axissymmetric flow CFD models that were developed using the commercial CFD code FLUENT. Figure 10. shows the experimentd and CFD analysis hot and cold temperature of air as a function of the CAMR. It can be seen that maximum hot outlet temperature of 90.8 ^{o}C (at 0.8 of CAMR) is obtained from CFD analysis and about 113 (at 0.89 of CAMR) is obtained from experiments. And a minimum cold outlet temperature of -22.6^{o}C (at 0.36 of CAMR) is obtained from CFD analysis and about -24.8 (at 0.30 of CAMR) is obtained from experiments. Thus CFD analysis is in reasonable agreement with experimental results.
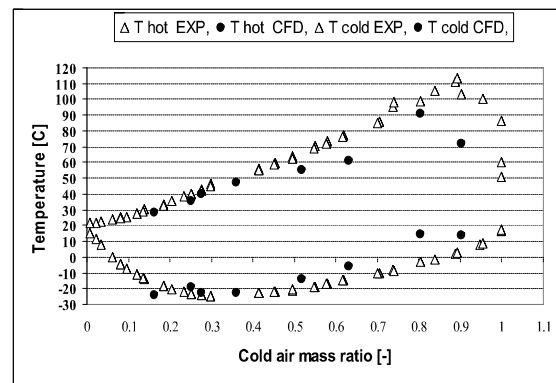

Figure. the experiment and CFD analysis hot and cold temperature of air as a function of the CAMR.

6. CONCLUSIONS

Experiment results of the temperature of the hot and cold air outlet of the vortex tube, with the CAMR and the pressure of the inlet air as parameters are presented. It is clear from our experiments that the higher the inlet pressure, the greater the temperature difference of the two outlet air streams. It is also shown that the CAMR is an important factor influence the performance of the vortex tube.

The results of experiment and CFD indicates that maximum hot air temperature is obtained for lower CAMR at the hot end and similarly lowest cold air temperature is obtained at lower CAMR at cold end (higher CAMR at hot end).

REFERENCES

[1] Ranque GJ, 1933, "Experiences sur la detente giratoire avec productions simultaneesd'un echappement d'air chand et d'un echappement d'air froid", *J Phys Radium*, Vol.4, pp. 112–4.

[2] Hilsch R, 1947, "The use of the expansion of gases in a centrifugal field as a cooling process", *Rev Sci Instrum*, Vol. 8, pp.108–13.

[3] Coccerill T, 1998, "Thermodynamics and Fluid Mechanics of a Ranque–Hisch Vortex Tube", Ph. D. Thesis, University of Cambridge.

[4] Lindstrom-Lang CU, 1964, "Gas Separation in the Ranque–Hisch Vortex Tube", *Int J Heat Mass Transfer*, Vol.7, pp. 1195–206.

[5] Kurosaka M, 1982, "Acoustic Streaming in Swirling Flow and the Ranque Hilsch Vortex Tube Effect", *J Fluid Mech*, Vol.124, pp.139–72.

[6] Ahlborn B, Keller JU, Rebhan E, 1998, "The Heat Pump in a Vortex Tube" *J Non- Equilib Thermodyn*, Vol. 23(2), pp. 159–65.

[7] Ahlborn BK, Gordon JM, 2000, "The Vortex Tube as a Classical Thermodynamic

Refrigeration Cycle", J Appl Phys, Vol.88(6), pp.3645–53.

[8] N.F. Aljuwayhel, G.F. Nellis, S.A. Klein, 2005, "Parametric and Internal Study of the Vortex Tube using a CFD model", *Int J Refrigeration* Vol. 28 (3), pp. 442–450.

[9] Saidi M H and Valipour M S, 20003, "Experimental modelling of vortex tube refrigerator". A*pplied thermal engineering*. Vol. 23, No. 15 pp 1971-1980.

[10] Stephan K, Lin S, Durst M, Hunag F and Seher D, 1983, "An investigation of Energy Separation in a Vortex Tube", *International Journal of Heat and Mass Transfer*, Vol. 26, No.3, pp 341-388.

[11] Ting-Quan MA, Qing-Guo, Jian YU, Fang YE, and Chong-Fang, 2002, "Experimental investigation on energy separation by vortex tubes". *12th international Heat Transfer Conference,*10, Paris.

[12] H. Takahama, and H. Yokosawa, 1981, "Energy Separation in Vortex Tubes with a Divergent Chamber", *ASME Journal of Heat Transfer*, Vol 103, pp. 196-203.

[13] H.H. Bruun, 1969, "Experimental Investigation of the Energy Separation in Vortex Tubes*", J Mech Eng Sci,* Vol. 11 (6), pp. 567–582.

[14] B. Ahlborn, J.U. Keller, R. Staudt, G. Treitz, R. Rebhan, 1994, "Limits of Temperature Separation in a Vortex Tube", *J Phys D: Appl Phys* 27, pp. 480–488.

[15] B.Ahlborn, J. Camire, J.U. Keller, 1996, "Low-Pressure Vortex Tubes", *J Phys D: Appl Phys,* Vol. 29, pp.1469–1472.

[16] W. Frohlingsdorf, H. Unger, 1999, "Numerical Investigations of the Compressible Flow and the Energy Separation in Ranque–Hilsch Vortex Tube", *Int. J. Heat Mass Transfer,* Vol. 42, pp. 415–422.

[17] Upendra Behera, P.J. Paul, S. Kasthurirengan, R. Karunanithi, S.N. Ram, K. Dinesh and S. Jacob, 2005, "CFD analysis and experimental investigations towards optimizing the parameters of Ranque–Hilsch vortex tube", *Int. J. Heat and Mass Transfer,* Vol. 48, Issue 10, 2005. pp. 1961-1973

[18] Jiří Linhart, Mohamad Kalal, Richard Matas, 2005, "Numerical study of vortex tube properties", *16th international symposium on transport phenomena*, 9, Prague